

# Effect of Common Faults on the Performance of Different Types of Vapor Compression Systems

Zhimin Du <sup>a,b</sup>, Piotr A. Domanski <sup>b,\*</sup> and W. Vance Payne <sup>b</sup>

<sup>a</sup> School of Mechanical Engineering, Shanghai Jiao Tong University, Shanghai, China

<sup>b</sup> HVAC&R Equipment Performance Group, National Institute of Standards and Technology,

100 Bureau Drive, MS 8631, Gaithersburg, MD 20899, USA

\*Phone: 1-301-975-5877; Email: piotr.domanski@nist.gov

## Abstract

The effect of faults on the cooling capacity, coefficient of performance, and sensible heat ratio, was analyzed and compared for five split and rooftop systems, which use different types of expansion devices, compressors and refrigerants. The study applied multivariable polynomial and normalized performance models, which were developed for the studied systems for both fault-free and faulty conditions based on measurements obtained in a laboratory under controlled conditions. The analysis indicated differences in responses and trends between the studied systems, which underscores the challenge to devise a universal FDD algorithm for all vapor compression systems and the difficulty to develop a methodology for rating the performance of different FDD algorithms.

**Keywords:** diagnostic efficiency; fault detection; fault diagnosis; normalized fault effect;  
vapor compression system

## Nomenclature

$a, b$	coefficient of multivariate polynomial
CA	condenser low airflow fault
COP	coefficient of performance
CVL	compressor valve leakage fault
$\Delta P_{LL}$	pressure drop in liquid line (kPa)
EA	evaporator low airflow fault
$F$	fault intensity
FXO	fixed orifice
LL	liquid line restriction fault
$\dot{m}$	refrigerant mass flow rate ( $\text{kg s}^{-1}$ )
$M$	refrigerant charge (kg)
OC	refrigerant overcharge fault
$Q$	cooling capacity (kW)
$R^2$	coefficient of determination
SHR	sensible heat ratio
$T$	temperature ( $^{\circ}\text{C}$ )
TXV	thermostatic expansion valve
UC	refrigerant undercharge fault
$\dot{V}$	volumetric airflow rate ( $\text{m}^3 \text{s}^{-1}$ )
$X$	operational parameter; COP, $Q$ , SHR, $T_{SC}$ , or $T_{SH}$
$\bar{X}$	– average value

$\hat{X}$  – value predicted by the model

$Y$  normalized figure of merit

### **Greek symbols**

$\phi_i$  fault defining parameter;  $\Delta P_{LL}$ ,  $M$ ,  $\dot{m}$ , or  $\dot{V}$

### **Subscripts**

cond condenser

evap evaporator

ID indoor air dry-bulb

IDP indoor air dew-point

OD outdoor air dry-bulb

SC subcooling

SH superheat

## **1. Introduction**

Since operational faults such as refrigerant undercharge, low airflow, or presence of noncondensable gases in the system may decrease the system capacity, increase energy consumption, and shorten the service life, early and correct fault detection and diagnosis (FDD) can provide economic and indoor comfort benefits. In general, an FDD protocol

requires specific measurements to be taken on the system and compares them with expected 'fault-free' values under given operating conditions and then, based on the difference between the measured and expected values or deviation patterns, the FDD protocol judges whether the operation is fault-free or faulty. If the system has been classified as faulty, the next challenge is a correct diagnosis of the fault.

Literature review indicates a significant interest in the FDD technology within the last twenty years. Examples of FDD studies include chillers [2-5], air handling units [6-9], split air-conditioning systems [10-12], and rooftop units [13-16]. Grace [17] studied the sensitivity of system performance to different refrigerant charge levels. Pak [18] investigated the impact of fouling and cleaning on heat exchanger performance. Ali [19] also investigated the effects of evaporator air-side fouling on system performance and indoor air quality. Palmiter [20] measured the effect of airflow and refrigerant charge faults on an air-source heat pump system charged with R410A. Yang [21] investigated the impact of evaporator fouling and filtration on the performance of packaged air conditioners. Through imposing a common single fault, Kim [11] and Yoon [22] investigated the performance of a residential heat pump in the cooling and heating modes, respectively. An electric utility [23] also extensively evaluated the effects of single and multiple common faults on a residential split system.

As FDD research left the infancy stage and matures for implementation in the market place, a concern can be voiced that there is no established metrics based on which the performance of a given FDD algorithm can be evaluated and relative performance merits of different FDD methods be expressed. It is also not clear what application limits should be observed to ensure robust performance of a specific FDD algorithm. Recently, Yuill and Braun [24, 25]

presented an interesting evaluation strategy for unitary vapor compression systems including rooftop units and split systems [24, 25]. The effectiveness of some popular FDD protocols applied to unitary systems was assessed in their research. Disappointedly, these FDD protocols didn't show reliable diagnostic capability or get satisfying scores during the evaluations, which indicated that these FDD protocols may be ineffective for the complex fault characteristics seen in field applications. Therefore, it is necessary to further investigate fault characteristics for different systems under various fault conditions to provide a useful reference for the design and development of a standardized evaluation strategy for FDD protocols.

In this study we developed multivariate polynomial and normalized performance to estimate the performance of vapor compression systems in the cooling mode under both fault-free and faulty conditions. Five different vapor compression systems – including both split and packaged rooftop systems – are examined. The effects of common faults for different refrigerants and systems equipped with different compressors and expansion devices are compared and analyzed.

## **2. System types and faults investigated**

Table 1 lists the five systems [26, 27] considered in this study. The table includes the main design features, which differentiate these systems and may affect their sensitivity to common faults: system type (split system and single-package rooftop), expansion device (thermostatic expansion valve [TXV] and fixed orifice [FXO]), compressor (reciprocating and scroll), and refrigerant (R410A and R407C). There are other design aspects that can affect the system's response to different faults, e.g., the evaporator and condenser size with

respect to the compressor size, relative sizes of the evaporator and condenser, the length of refrigerant lines connecting the indoor and outdoor section (in case of a split system). These design aspects will not be included in our analysis because of the lack of detailed information.

Below are the definitions of six common faults considered in this study.

Refrigerant Undercharge/Overcharge (UC or OC): The mass of refrigerant in the system,  $M$ , is smaller/larger than the nominal mass recommended by the manufacturer.

Evaporator low indoor airflow (EA): The evaporator airflow,  $\dot{V}_{evap}$ , is lower than the manufacturer's recommended nominal value.

Condenser low outdoor airflow (CA): The condenser airflow,  $\dot{V}_{cond}$ , is lower than the manufacturer's recommended nominal value.

Compressor valve leakage (CVL): The refrigerant mass flow rate through the system,  $\dot{m}$ , is lower than the fault-free value. This fault is typically simulated in experimental studies by installing a hot-gas bypass between the discharge-side and suction-side of the compressor.

Liquid line restriction (LL): The pressure drop in the liquid line between the condenser outlet and the expansion device inlet,  $\Delta P_{LL}$ , is greater than the fault-free value.

The fault intensity ( $F_i$ ) for these faults is calculated by dividing the difference between the faulty and fault-free value of the pertinent parameter by the fault-free value, as shown in Eq. 1.

$$F_i = \frac{\phi_{i,fault} - \phi_{i,fault-free}}{\phi_{i,fault-free}} \cdot 100 \% \quad (1)$$

where the index  $i$  denotes a specific fault, UC, OC, EA, CA, CVL, or LL, and pertinent fault defining parameters are  $\phi_{UC} = M$ ,  $\phi_{OC} = M$ ,  $\phi_{EA} = \dot{V}_{evap}$ ,  $\phi_{CA} = \dot{V}_{cond}$ ,  $\phi_{CVL} = \dot{m}$ , and  $\phi_{LL} = \Delta P_{LL}$ , respectively. Table 2 shows faults and fault intensities for which experimental data are available for the studied systems [26, 27].

### 3. Performance models for vapor compression systems

#### 3.1 Multivariate polynomial models for fault-free operation

We used multivariable polynomial models for representing the performance of the studied systems following the analysis of different model categories presented by Kim et al. [28]. Since multivariate polynomial models do not consider the physics of the systems, they require sufficient data to ensure their prediction accuracy. The higher the order, the larger the amount of training data required. On the other hand, 1<sup>st</sup> order multivariate polynomial models usually do not provide good prediction accuracies for vapor compression systems. The evaluation of example cases showed that the 2<sup>nd</sup> order multivariate polynomial model is the most suitable for use in this study because of its simplicity and acceptable predictions with the limited performance data available.

Equation 2 shows the general form of the 2<sup>nd</sup> order multivariate polynomial model for the  $i^{th}$  dependent variable. The dependent variables can be regressed upon the database generated from the fault-free experimental tests. The outdoor air dry-bulb temperature ( $T_{OD}$ ), indoor air dry-bulb temperature ( $T_{ID}$ ) and indoor air dew-point temperature ( $T_{IDP}$ ) are the independent variables.

$$X = a_0 + a_1 T_{OD} + a_2 T_{ID} + a_3 T_{IDP} + a_4 T_{OD} T_{ID} + a_5 T_{ID} T_{IDP} + a_6 T_{OD} T_{IDP} + a_7 T_{OD}^2 + a_8 T_{ID}^2 + a_9 T_{IDP}^2 \quad (2)$$

where  $X$  represents a system operational parameter such as cooling capacity ( $Q$ ), coefficient of performance (COP), sensible heat ratio (SHR), evaporator superheat ( $T_{SH}$ ), or condenser subcooling ( $T_{SC}$ ).

### 3.2 Normalized performance models for faulty operation

When faults occur in a vapor compression system, the capacity, COP, and SHR deviate from their fault-free values. This performance deviation is expressed non-dimensionally by Eq. 3 [29].

$$Y = \frac{X_{fault}}{X_{fault-free}} \quad (3)$$

where  $Y$  is the figure of merit and  $X$  denotes the operational parameter for the faulty and fault-free operation, as indicated by the subscripts. These deviations depend on the type of fault, fault intensity, and operating conditions, and can be correlated using the following 2<sup>nd</sup> order polynomial [29]:

$$Y = \frac{X_{fault}}{X_{fault-free}} = 1 + (b_0 + b_1 T_{OD} + b_2 T_{ID} + b_3 F)F \quad (4)$$

### 3.3 Statistical evaluation of fault-free and fault models

The coefficient of determination,  $R^2$  (Eq. 5), provides a measure of goodness for the developed correlation.

$$R^2 = 1 - \frac{\sum_{i=1}^n (X_i - \hat{X}_i)^2}{\sum_{i=1}^n (X_i - \bar{X}_i)^2} \quad (5)$$

Table 3 presents  $R^2$  values of the developed models for capacity, COP, and SHR for the five

studied systems for fault-free operation and operation under the UC, OC, EA, and CA faults. Empty entries in the System III and System V columns denote the parameters for which insufficient data prevented the development of the model. In general,  $R^2$  values for the fault-free operation are better (higher) than those for the operation under different faults. While experimental data for both fault-free and faulty operation are burdened by the same fundamental measurement uncertainties, measurements for the faulty operation are additionally burdened by the uncertainty of imposing a fault of the intended level of intensity. Also, in most cases the number of tests performed for the faulty operation is smaller than that for the fault-free operation. All these factors are reflected in  $R^2$  values, which are typically lower for the operation under faults than those for fault-free tests.

Typical uncertainties for psychrometric measurements are on the order of 5 % of the measured values at a 95 % confidence level when measurements are made according to ASHRAE Standards [30]. For System I, the uncertainty of the cooling capacity and COP were 4.0 % and 5.5 %, respectively [28]. If we use 5 % of the value as a representative uncertainty for our normalized performance correlation, the overall uncertainty will be approximately 7 % for the calculated  $Y$  values (Eq. 4).

#### **4. Effect of faults on performance**

##### **4.1 Fault effects on the reference system**

For the purpose of this comparative study we selected System I as a reference system because it is a typical split residential heat pump equipped with a TXV, and its fault-free and faulty performance has been broadly measured during laboratory tests with six faults at various fault

intensities. Figure 1 presents the capacity, COP, and SHR for System I operating under different single faults. The presented data include experimental results (discrete points) and model predictions (continuous lines) using the equations indicated in Table 3 for the fault-free and faulty operation. The lines are only shown over the range of the data with no extrapolation; this is intended to show the limits of the data and our reluctance to extrapolate outside of the available data range. The figure uses a non-dimensional scale for the presented parameters where the faulty values are normalized with respect to their fault-free counterparts. The effect of studied faults on the capacity differs. For five out of six faults – refrigerant overcharge fault (OC) being the exception – the capacity decreases with increasing fault intensity, showing a wide variation of capacity degradation rate depending on the fault. The OC fault can increase the capacity when the fault intensity is within the 0 % - 20 % range. For intensities greater than 20 %, the capacity decreases.

The COP – on the other hand – consistently decreases with increasing fault intensities greater than 15 % under all fault scenarios. The CVL, CA, and UC faults can degrade the COP the most. Regarding the SHR, the EA fault decreases it (which means an improvement in moisture removal), and the CVL and CA faults increase it. Other faults have a less than 10 % effect on the SHR at the largest intensities studied.

Evaporator superheat and condenser subcooling are two features commonly used for FDD because of their sensitivity to some common faults and their ease of measurement. Figure 2 shows changes in  $T_{SH}$  and  $T_{SC}$  for System I operating with six single faults. The refrigerant UC fault can greatly affect  $T_{SH}$  if its intensity exceeds 10 %. The LL fault may also increase  $T_{SH}$  markedly for intensities greater than 20 %. Other faults do not affect  $T_{SH}$  more than

$\pm 10\%$ ; their effect on superheat can be considered neutral.

The UC fault strongly affects the condenser subcooling, which can be lost at 20 % refrigerant undercharge. Also, the CA and OC faults have a greater than 10 % effect on subcooling (negative and positive, respectively). The remaining faults tend to reduce the subcooling although their influence over the range of data is not as pronounced.

We need to emphasize that the above trends for  $T_{SH}$  and  $T_{SC}$  were measured on a system equipped with a TXV, and they are not exactly applicable to a system using a FXO. To contrast the differences, Table 4 presents diagnostic rules for  $T_{SH}$  and  $T_{SC}$  reported for a TXV-equipped split system [31] and a rooftop air conditioner equipped with a FXO [32]. The diagnostic rules for the FXO-equipped air conditioner do not agree in several cases with those listed for the TXV-equipped systems. In most instances the neutral trend for the TXV-equipped system contrasts a positive or negative trend indicated for the FXO-equipped system.

#### **4.2 Comparison of fault effects on systems of different design**

Although common air conditioners are built on the vapor-compression principle, their response to common faults may differ due to differences in their overall design or component selection. Hence, it is of interest to compare performance of different system operating under faults having in mind the design aspects that are the same and those that are different for the compared equipment. The comparisons presented below are limited to the available fault data range with no extrapolation. In a few cases the presented graphical results for

compared systems are for somewhat different operating indoor and outdoor temperatures, as indicated in the figures. This was done out of necessity since performance data under faults are very scarce, and they are not collected according to established test metrics by different researchers. Although we used operating conditions that are not exactly the same, they seem to be close enough and adequate for learning about the effects of different faults and for reaching the qualitative conclusions we are seeking to make.

#### ***4.2.1 Systems with different compressors: System I (scroll) and System II (reciprocating)***

In this comparison case we considered Systems I and II, which use a scroll and reciprocating compressors, respectively. Otherwise, both units are split systems equipped with a TXV and charged with R410A. Generally, the capacity and COP trends of System I and System II are similar when UC, OC, EA and CA faults are imposed: the capacity and COP fall, and the differences in their degradation degrees are statistically insignificant (Figures 3, 4, 5, and 6). As for the SHR, its trend is within a 10 % band between Systems I and II with some dissimilarity for the UC fault, where the SHR of System II (reciprocating compressor) seems to not be affected by the fault while the SHR for System I increases with the fault intensity.

A review of  $T_{SH}$  and  $T_{SC}$  data for Systems I and II showed that their pattern for the UC, OC, EA, and CA faults was the same as that presented in Table 4 for a split/TXV system for all cases except the  $T_{SC}$  trend for System II under the CA fault (zone  $T_{SH} < 9$  °C), which was neutral instead of being negative. The following are the  $T_{SH}$  and  $T_{SC}$  trends for which there was no deviation from Table 4: the UC fault (zone  $T_{SH} > 9$  °C),  $T_{SH} \uparrow$ ,  $T_{SC} \downarrow$ ; the OC fault

(zone  $T_{SH} < 9\text{ }^{\circ}\text{C}$ ),  $T_{SH} \sim$ ,  $T_{SC} \uparrow$ ; and the EA fault (zone  $T_{SH} < 9\text{ }^{\circ}\text{C}$ ),  $T_{SH} \sim$ ,  $T_{SC} \sim$ .

While the  $T_{SH}$  and  $T_{SC}$  patterns are the same for both systems, the value of residuals can be substantially different, which can affect detection and diagnostic robustness of applied FDD protocols. For example, operating at similar conditions with an OC fault of 10 % intensity, the residual of  $T_{SC}$  for System II was 3.4 °C (large positive), as opposed to 0.6 °C (small positive) for System I. The 0.6 °C residual will be disregarded by the FDD protocol if the diagnostic threshold for the OC fault is set to 1.0 °C. Hence, in this case, System II would be diagnosed for the OC fault while System I would not. Detail design data on Systems I and II were not available to explore whether some design features, e.g., different internal volumes of system components, contributed to the observed different  $T_{SC}$  residuals.

#### ***4.2.2 Systems with different expansion devices: System II (TXV) and III (FXO)***

Differences in the diagnosis rules presented in Section 4.1 for TXV-equipped and FXO-equipped systems already indicated differences in responses to faults by these systems. Figures 7, 8 and 9 present more detailed information about the performance characteristics of System II and System III, which use a TXV and FXO, respectively. Besides different expansion devices, both units are split systems, both use reciprocating compressors, and both are charged with R410A.

The capacity and COP decrease with increasing intensities of UC, EA, and CA faults for both systems, but the rate of performance degradation is significantly sharper for the UC fault for System III (FXO) than for System II (TXV). The SHR of the TXV-equipped unit is not affected by the UC fault while it is increasing for the FXO-equipped unit, which implies

reduced moisture removal capability. For the EA and CA faults, the SHR characteristics are fairly similar with SHR falling and increasing for the EA and CA faults, respectively.

It is of interest to compare  $T_{SH}$  and  $T_{SC}$  patterns of System II (TXV) and of System III (FXO) operating under various faults. They are different. The pattern of System II is consistent with that shown in Table 4 for a TXV-equipped split system for the UC, CA, and EA faults. For the CA fault (zone  $T_{SH} < 9$  °C) there is a discrepancy: the measured  $T_{SC}$  trend is neutral instead of being negative.

The patterns of System III (FXO) are better aligned with that of a rooftop unit with a FXO in Table 4 even though it is a split type: the  $T_{SH}$  and  $T_{SC}$  pattern is the same for the UC fault for the whole range of fault intensity. The EA and CA faults produce the same patterns at intensities greater than 25 %. This observation indicates that the expansion device plays an essential role in the feature characteristics of vapor compression systems and may influence the system performance much more than the overall system design.

#### ***4.2.3 Systems with different refrigerants: System IV (R410A) and V (R407C)***

For this comparison we used System IV and System V charged with R410A and R407C, respectively. Otherwise, both systems are single-package rooftop units using the same type of compressor (scroll) and expansion device (FXO). We need to note that R410A and R407C have significantly different thermodynamic properties; although both are zeotropic mixtures, the two-phase glide of R410A is negligible (within 0.5 K) while the glide of R407C is substantial (approximately 4 K, depending on the pressure). Besides the difference in the two-phase glide, operating pressures of R410A are substantially higher than those of R407C.

The degradation of capacity due to the UC fault is very similar for both systems; however, the degradation of COP for System IV (R410A) is more severe and results in a 10 % lower value compared to that of System V (R407C) for fault intensities greater than 15 % (Figure 10).

For an OC fault, the data showed a small increase in capacity of System V (R407C), which is a typical response to refrigerant overcharging, and a small decrease in capacity of System IV (R410A) (Figure 11). While both systems experienced COP degradation, the drop in the COP of System IV (R410A) is much more severe.

The COPs of both systems were similarly degraded by the condenser low airflow (CA fault) (Figure 12). However, the impact of this fault on the capacity and SHR was relatively small on the R407C system compared to the R410A system.

Review of the  $T_{SH}$  and  $T_{SC}$  data for Systems IV and V showed that their pattern was identical for all faults. With respect to the pattern for the rooftop/FXO system presented in Table 4, the patterns agreed for the UC, EA, and CA faults for all cases except the  $T_{SC}$  trend for the CA fault, which was neutral for both systems and contrasted the negative trend shown in Table 4. For the OC fault (not represented in the table for the rooftop/FXO system), both systems showed the same trend,  $T_{SH} \downarrow$  and  $T_{SC} \uparrow$ , which can be expected for all systems equipped with a FXO.

## **5. Conclusions**

We analyzed effects of four common faults on five different vapor compression systems operating in the cooling mode based on experimental data obtained in a laboratory under controlled operating conditions. The systems differed by the design type (split and

single-package rooftop), compressor (scroll and reciprocating), expansion device (TXV and FXO) and refrigerant (R410A and R407C). We noted different fault effects on the systems' capacity, COP, and SHR. The expansion device type had the strongest impact on performance characteristics under different faults. The impact of the compressor type was the smallest; the observed differences could possibly be a result of a combination of effects of several design aspects and measurement uncertainty.

We also noted differences in the trends for evaporator superheat and condenser subcooling, for the studied systems and those presented in the literature in the form of FDD diagnostic rules. Since the evaporator superheat and condenser subcooling are the most commonly used features by FDD methods, the observed differences in the pattern of these features point to the inherent challenge of developing a universal FDD algorithm for all vapor compression systems as well as to the difficulty of developing a general methodology for rating different FDD methods.

### **Acknowledgements**

The authors acknowledge Prof. J. Braun for sharing FDD experimental data taken at Purdue University, and Drs. D. Yuill and H. Cheung for their helpful interactions.

## References:

- [1] G.J. Vachtsevanos, F.L. Lewis, M.J. Roemer, A. Hess, B. Wu, Intelligent fault diagnosis and prognosis for engineering systems, Hoboken, NJ, Wiley, 2006
- [2] M.C. Comstock, J.E. Braun, E.A. Groll, The sensitivity of chiller performance to common Faults, *HVAC&R Research*, 2001, 7(3): 263-279
- [3] T.A. Reddy, Development and evaluation of a simple model-based automated fault detection and diagnosis (FDD) method suitable for process faults of large chillers, *ASHRAE Transactions*, 2007, 113(2): 27-39
- [4] X. Zhao, M. Yang, H. Li, Decoupling features for fault detection and diagnosis on centrifugal chillers (1486-RP), *HVAC&R Research*, 2011, 17(1): 86-106
- [5] S.W. Wang, J.T. Cui, Sensor-fault detection, diagnosis and estimation for centrifugal chiller systems using principal-component analysis method, *Applied Energy*, 2005, 82 (3): 197-213
- [6] L.K. Norford, J.A. Wright, R.A. Buswell, D. Luo, C. Klaassen, A. Suby, Demonstration of fault detection and diagnosis methods for air-handling units (ASHRAE 1020-RP), *HVAC&R Research*, 2002, 8(1): 41-72
- [7] J. Schein, S.T. Bushby, N.S. Castro, J.M. House, A rule-based fault detection method for air handling units, *Energy and Buildings*, 2006, 38 (12): 1485-1492
- [8] S.W. Wang, J.Y. Qin, Sensor fault detection and validation of VAV terminals in air-conditioning systems, *Energy Conversion and Management*, 2005, 46(15-16): 2482-2500
- [9] Z.M. Du, X.Q. Jin, X.B. Yang, A robot fault diagnostic tool for flow rate sensors in air

- dampers and VAV terminals, *Energy and Buildings*, 2009, 41(3): 279-286
- [10] M. Kim, S.H. Yoon, W.V. Payne, P.A. Domanski, Design of a steady-state detector for fault detection and diagnosis of a residential air conditioner. *International Journal of Refrigeration*, 2008, 31(5): 790-799
- [11] M. Kim, W.V. Payne, P.A. Domanski, S.H. Yoon. Performance of a residential heat pump operating in the cooling mode with single faults imposed, *Applied Thermal Engineering*, 2009, 29: 770-778
- [12] J. Heo, W.V. Payne, P.A. Domanski, FDD CX: A fault detection and diagnostic commissioning tool for residential air conditioners and heat pumps, *NIST Technical Note 1774*, National Institute of Standards and Technology, Gaithersburg, MD, USA, 2012
- [13] H. Li, J.E. Braun, An improved method for fault detection and diagnosis applied to packaged air conditioners, *ASHRAE Transactions*, 2003, 109(2): 683-692
- [14] P.R. Armstrong, C.R. Laughman, S.B. Leeb, L.K. Norford, Detection of rooftop cooling unit faults based on electrical measurements, *HVAC&R Research*, 2006, 12(1): 151-175
- [15] B. Chen, J.E. Braun, Simple rule-based methods for fault detection and diagnostics applied to packaged air conditioners, *ASHRAE Transactions*, 2001, 107(1): 837-847
- [16] H. Li, J.E. Braun, Decoupling features and virtual sensors for diagnosis of faults in vapor compression air conditioners, *International Journal of Refrigeration*, 2007, 30(3): 546-564
- [17] I.N. Grace, D. Datta, S.A. Tassou, Sensitivity of refrigeration system performance to

- charge level and parameters for on-line leak detection, *Applied Thermal Engineering*, 2005, 25(4): 557-566
- [18] B.C. Pak, E.A. Groll, J.E. Braun, Impact of fouling and cleaning on plate fin and spine fin heat exchanger performance. *ASHRAE Transactions*, 2005, 111(1): 496-504
- [19] A.H.H. Ali, I.M. Ismail, Evaporator air-side fouling: effect on performance of room air conditioners and impact on indoor air quality, *HVAC&R Research*, 2008, 14(2): 209-219
- [20] L. Palmiter, J-H Kim, B. Larson, P.W. Francisco, E.A. Groll, J.E. Braun, Measured effect of airflow and refrigerant charge on the seasonal performance of an air-source heat pump using R-410A, *Energy and Buildings*, 2011, 43: 1802-1810
- [21] L. Yang, J.E. Braun, E.A. Groll, The impact of evaporator fouling and filtration on the seasonal performance of an air-source heat pump using R-410A, *Energy and Buildings*, 2011, 43: 1802-1810
- [22] S.H. Yoon, W.V. Payne, P.A. Domanski, Residential heat pump heating performance with single faults imposed, *Applied Thermal Engineering*, 2011, 31: 765-771
- [23] Southern California Edison, Design and Engineering Services, HT.11.SCE.007: Evaluating the effects of common faults on a residential split system, 2012
- [24] D.P. Yuill, J.E. Braun, Evaluating fault detection and diagnostics protocols applied to air-cooled vapor compression air conditioners, *Proceedings of the 14th International Refrigeration and Air Conditioning Conference at Purdue*, West Lafayette, IN, 2012, July 16-19, Paper 2470
- [25] D.P. Yuill, J.E. Braun, Evaluating the performance of fault detection and diagnostics

- protocols applied to air-cooled unitary air-conditioning equipment, *HVAC&R Research*, 2013, 19(7): 882-891
- [26] J.E. Braun, H. Cheung, D.P. Yuill, Development of an Evaluation System for Fault Detection and Diagnosis Tools Applied to Vapor Compression Air-Conditioning Systems, *NIST Grant #: 60NANB11D153*, National Institute of Standards and Technology, Gaithersburg, MD, USA
- [27] David P. Yuill, Development of methodologies for evaluating performance of fault detection and diagnostics protocols applied to unitary air-conditioning equipment, Ph.D. Dis. Purdue University, West Lafayette, Indiana, 2014. Print
- [28] M. Kim, W.V. Payne, P.A. Domanski, Performance of a residential heat pump operating in the cooling mode with single faults imposed, *NISTIR 7350*, National Institute of Standards and Technology, Gaithersburg, MD, USA, 2006
- [29] J.M. Cho, J. Heo, W.V. Payne, P.A. Domanski, Normalized performance parameters for a residential heat pump in the cooling mode with single faults imposed, *Applied Thermal Engineering*, 2014, 67: 1-15
- [30] ASHRAE Standard 37, Methods of testing for rating electrically driven unitary air conditioning and heat pump equipment, 2009
- [31] M. Kim, S.H. Yoon, W.V. Payne, P.A. Domanski, Cooling mode fault detection and diagnosis method for a residential heat pump, *NIST Special Publication 1087*, National Institute of Standards and Technology, USA, 2008

- [32] M.S. Breuker, J.E. Braun, Evaluating the performance of a fault detection and diagnostic system for vapor compression equipment, *HVAC&R Research*, 1998, 4(4): 401-425

## Figures

Figure 1. Capacity, COP, and SHR of System I with faults

Figure 2. Evaporator superheat and condenser subcooling of System I with faults

Figure 3. Capacity, COP and SHR of System I (scroll compressor) and System II (reciprocating compressor) operating with UC fault

Figure 4. Capacity, COP and SHR of System I (scroll compressor) and System II (reciprocating compressor) operating with OC fault

Figure 5. Capacity, COP and SHR of System I (scroll compressor) and System II (reciprocating compressor) operating with EA fault

Figure 6. Capacity, COP and SHR of System I (scroll compressor) and System II (reciprocating compressor) operating with CA fault

Figure 7. Capacity, COP and SHR of System II (TXV) and System III (FXO) operating with UC fault

Figure 8. Capacity, COP and SHR of System II (TXV) and System III (FXO) operating with EA fault

Figure 9. Capacity, COP and SHR of System II (TXV) and System III (FXO) operating with CA fault

Figure 10. Capacity, COP and SHR of System IV (R410A) and System V (R407C) operating with UC fault

Figure 11. Capacity, COP and SHR of System IV (R410A) and System V (R407C) operating with OC fault

Figure 12. Capacity, COP and SHR of System IV (R410A) and System V (R407C) operating with CA fault

## Tables

**Table 1. System descriptions**

No.	System Type	Capacity (kW)	Expansion Device	Compressor	Refrigerant
I	Split	8.8	TXV	Scroll	R410A
II	Split	10.6	TXV	Reciprocating	R410A
III	Split	10.6	FXO	Reciprocating	R410A
IV	Rooftop	10.6	FXO	Scroll	R410A
V	Rooftop	17.6	FXO	Scroll	R407C

**Table 2. Fault intensities for the studied systems**

System	Faults					
	UC	OC	EA	CA	CVL	LL
I	-30 % ~ -10 %	10 % ~ 30 %	-32 % ~ -6 %	-50 % ~ -5 %	2.5 % ~ 38 %	0.7 % ~ 32 %
II	-39 % ~ -8 %	13 % ~ 42 %	-57 % ~ 40 %	-69 % ~ -10 %	-	-
III	-43 % ~ -4 %	-	-42 % ~ 13 %	-69 % ~ -7 %	-	-
IV	-42 % ~ -3 %	5 % ~ 30 %	-64 % ~ 38 %	-45 % ~ -4 %	-	-
V	-36 % ~ -10 %	9 % ~ 29 %	-	-27 % ~ -7 %	-	-

**Table 3. Coefficients of determination ( $R^2$ ) for  $Q$ , COP, and SHR**

		System I	System II	System III	System IV	System V
<b>Fault-free</b> <b>(Eq. 2)</b>	$Q$	0.996	0.990	0.999	0.993	0.994
	<b>COP</b>	0.997	0.995	0.999	0.998	0.998
	<b>SHR</b>	0.999	0.993	0.999	0.990	0.997
<b>UC</b> <b>Fault</b> <b>(Eq. 4)</b>	$Q$	0.991	0.998	0.897	0.990	0.994
	<b>COP</b>	0.988	0.995	0.998	0.987	0.993
	<b>SHR</b>	0.886	0.846	0.830	0.859	0.889
<b>OC</b> <b>Fault</b> <b>(Eq. 4)</b>	$Q$	0.994	0.963	-	0.956	0.931
	<b>COP</b>	0.909	0.949	-	0.962	0.901
	<b>SHR</b>	0.843	0.958	-	0.893	0.917
<b>EA</b> <b>Fault</b> <b>(Eq. 4)</b>	$Q$	0.930	0.904	0.987	0.963	-
	<b>COP</b>	0.918	0.872	0.983	0.923	-
	<b>SHR</b>	0.901	0.809	0.998	0.956	-
<b>CA</b> <b>Fault</b> <b>(Eq. 4)</b>	$Q$	0.976	0.991	0.959	0.969	0.990
	<b>COP</b>	0.983	0.996	0.975	0.992	0.999
	<b>SHR</b>	0.973	0.991	0.991	0.932	0.871

**Table 4. Diagnosis rules of  $T_{SH}$  and  $T_{SC}$  for TXV- and FXO-equipped systems**

System	Zones	Feature	UC	OC	EA	CA	CVL	LL
<b>Split with TXV [31]</b>	$T_{SH} < 9$	$T_{SH}$	~	~	~	~	~	~
		$T_{SC}$	↓	↑	~	↓	↓	~
	$T_{SH} > 9$	$T_{SH}$	↑	not given	not given	↑	not given	↑
		$T_{SC}$	↓	not given	not given	↓	not given	↑
<b>Rooftop with FXO [32]</b>	<b>one zone</b>	$T_{SH}$	↑	not given	↓	↓	↓	↑
		$T_{SC}$	↓	not given	↓	↓	↓	↑

Note: ↑ = positive; ↓ = negative; ~ = neutral

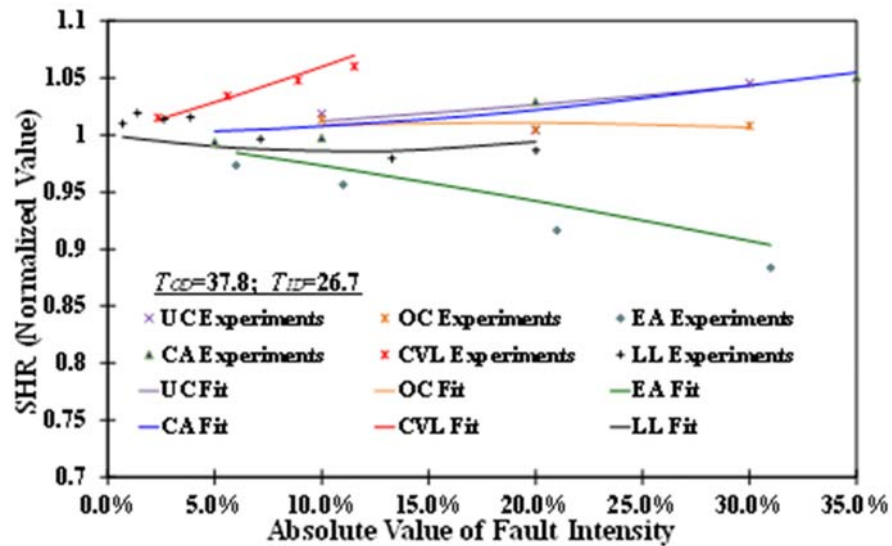
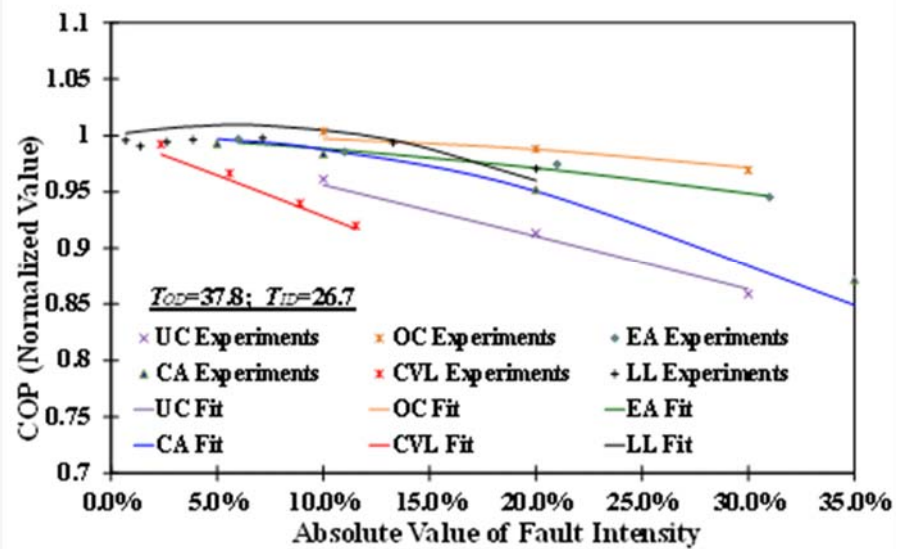
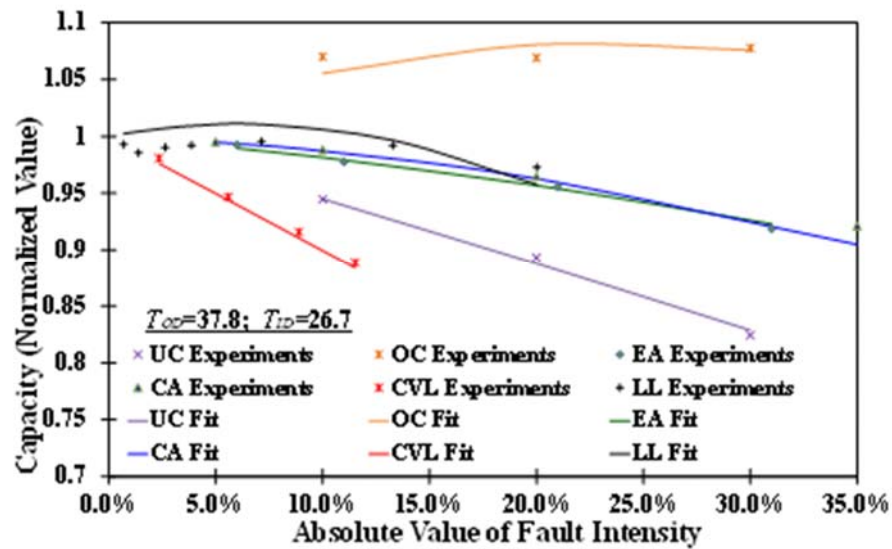


Figure 1.

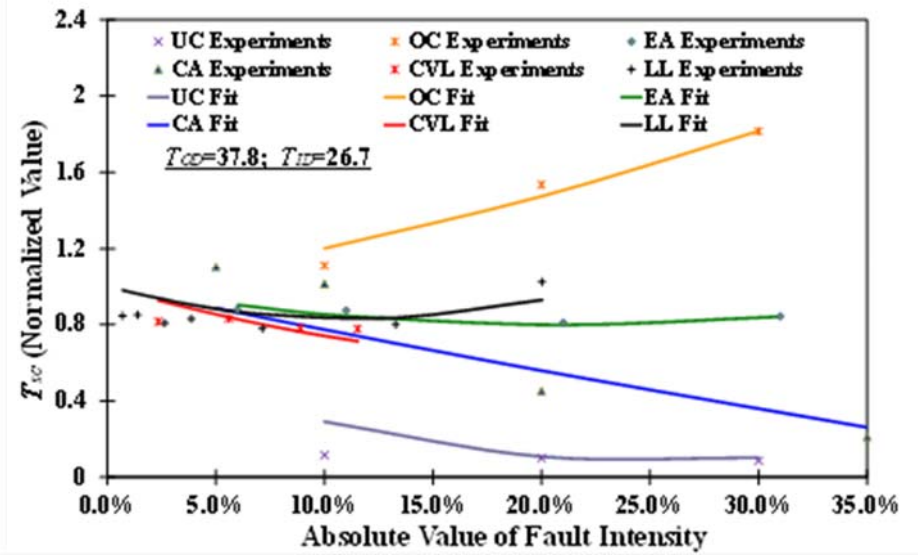
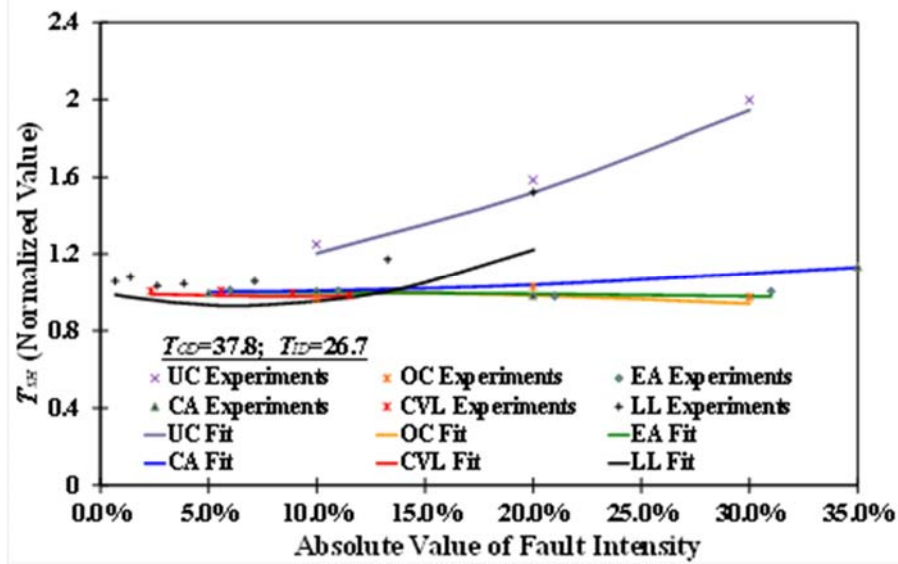


Figure 2.

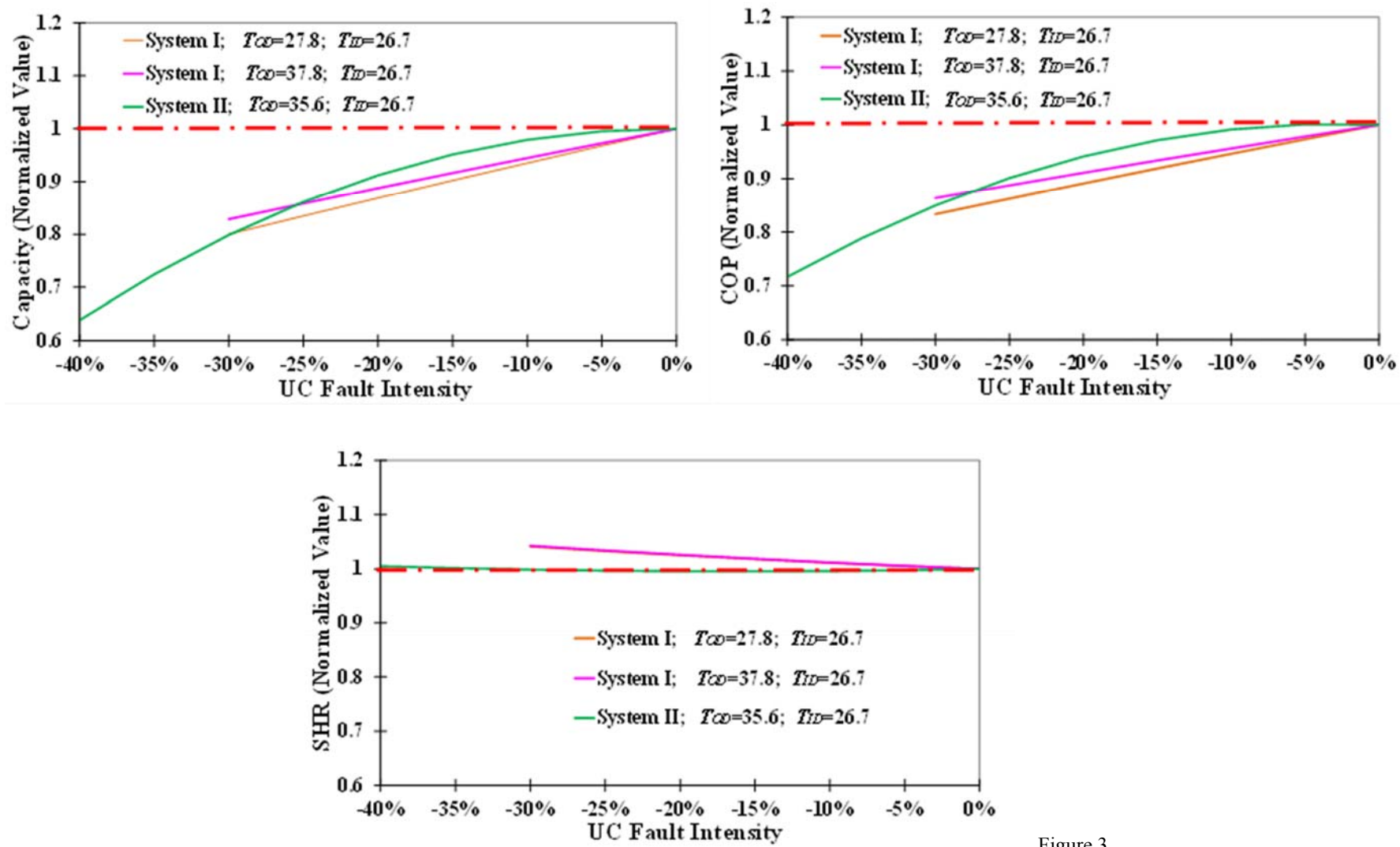


Figure 3.

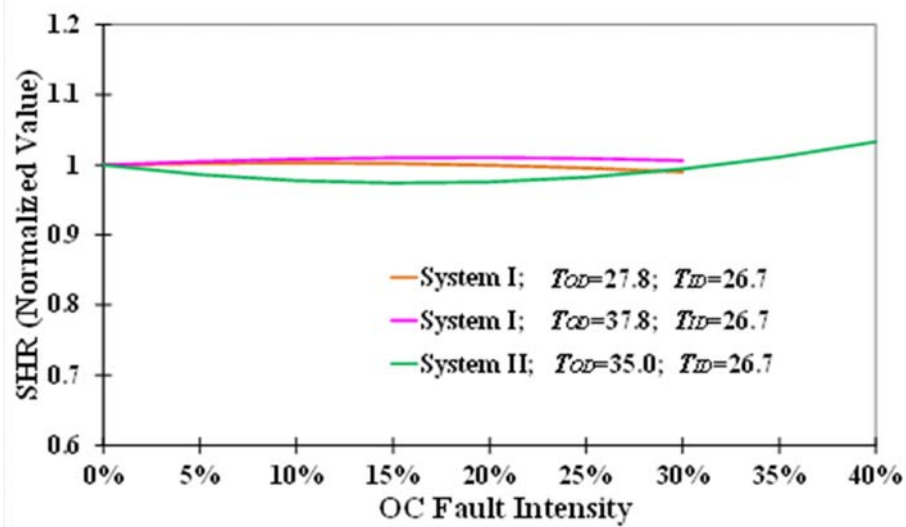
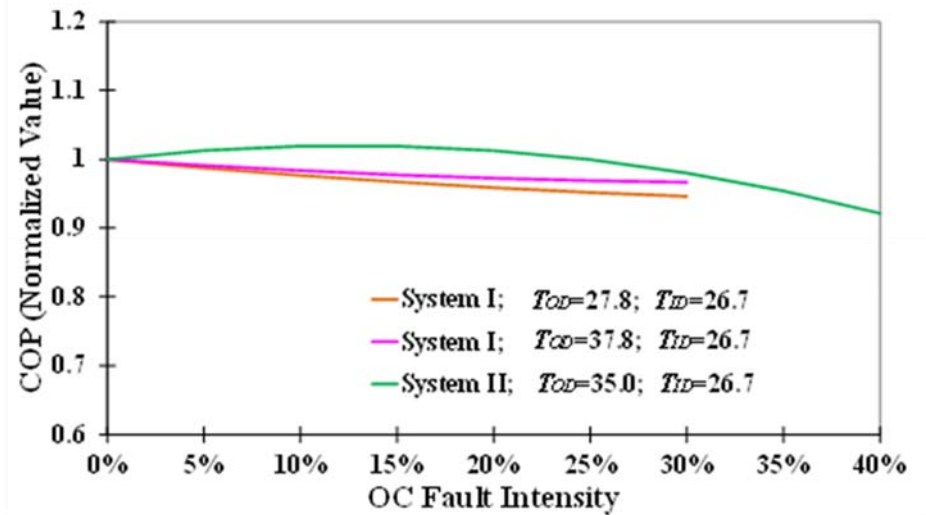
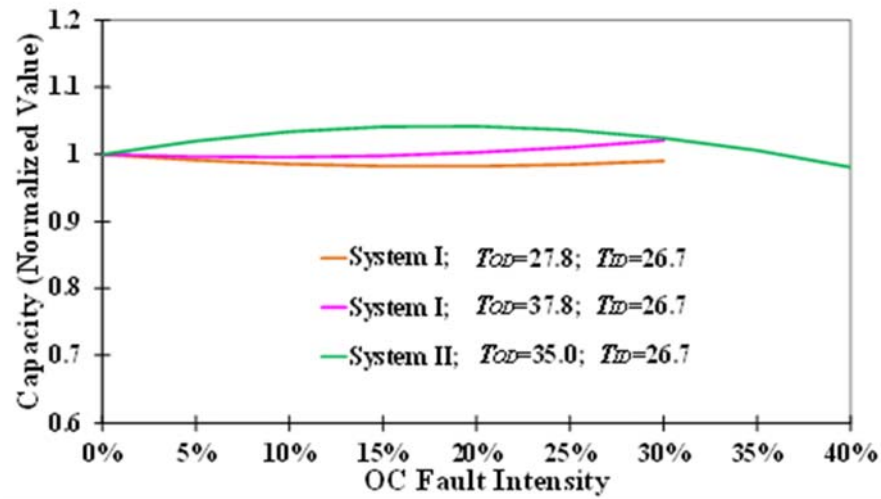


Figure 4

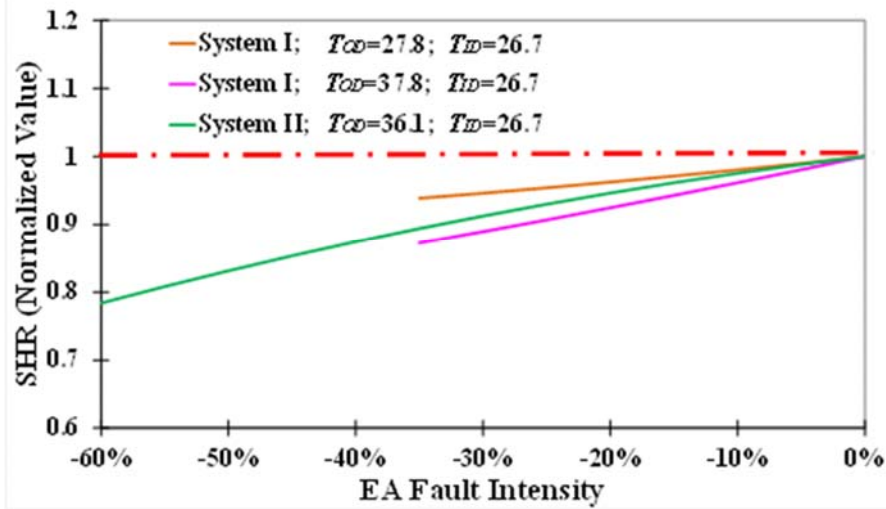
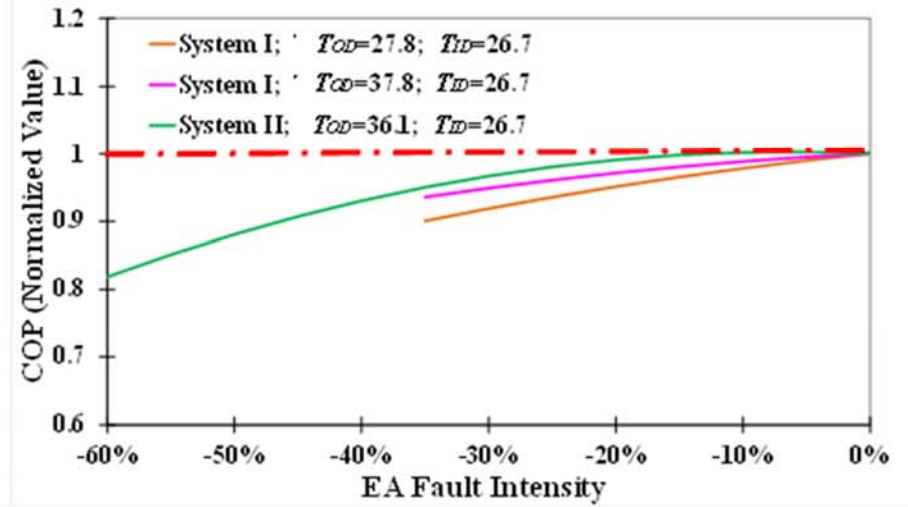
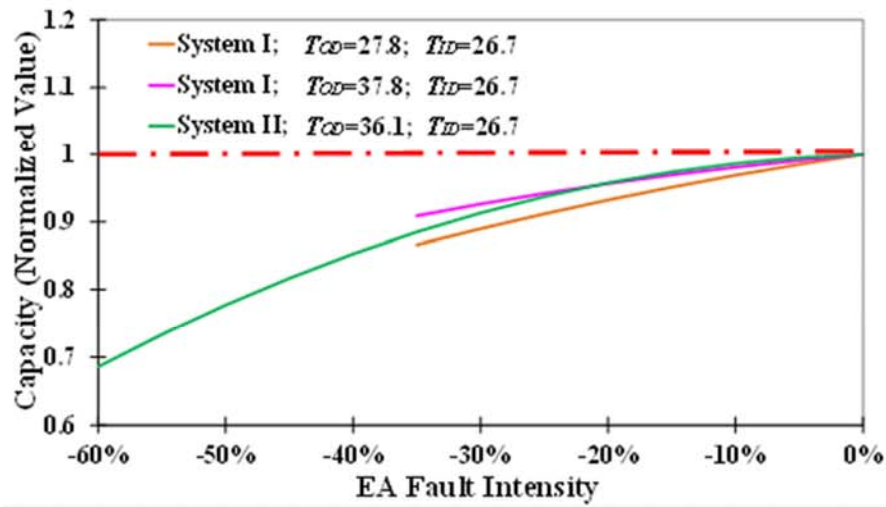


Figure 5

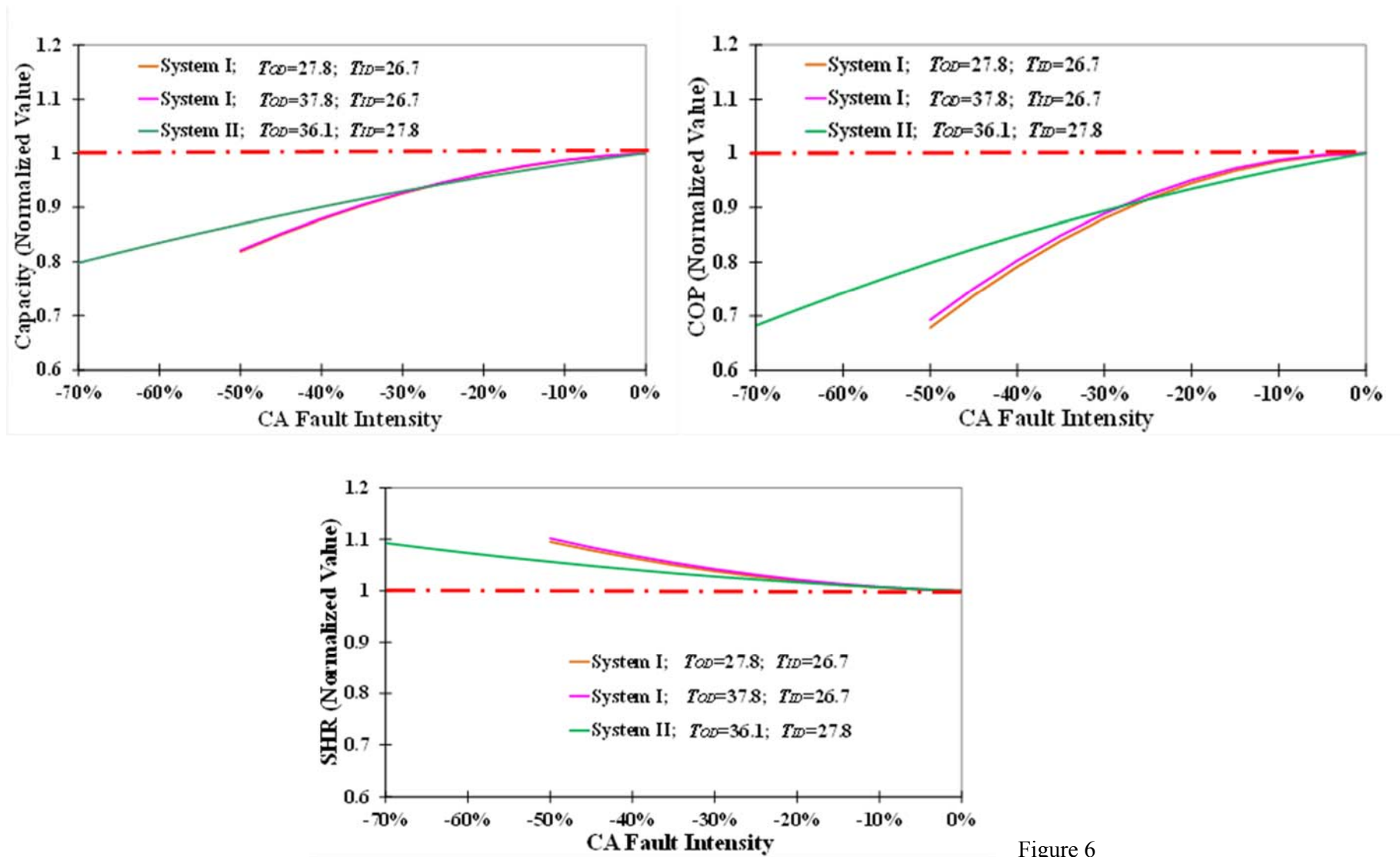


Figure 6

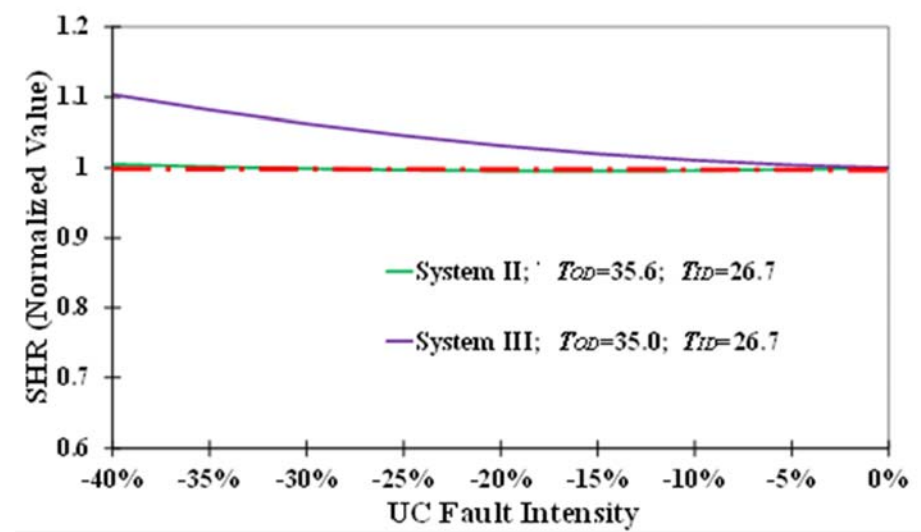
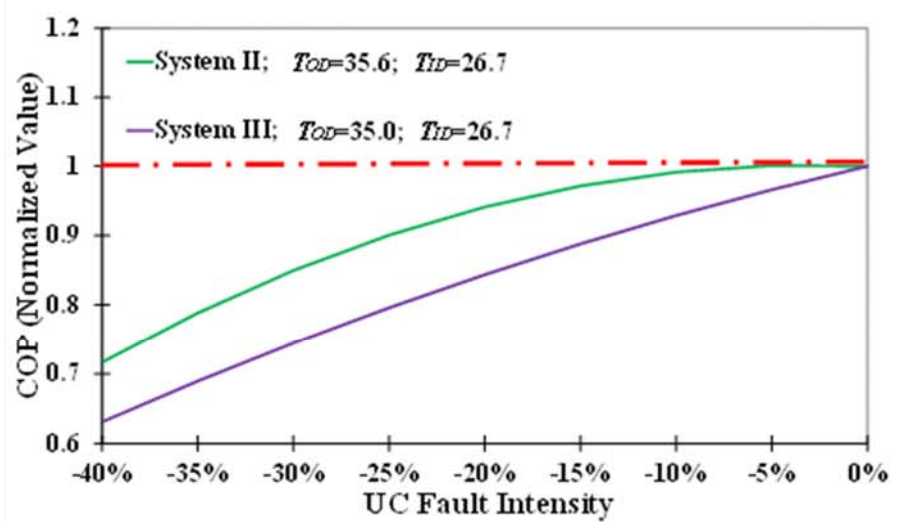
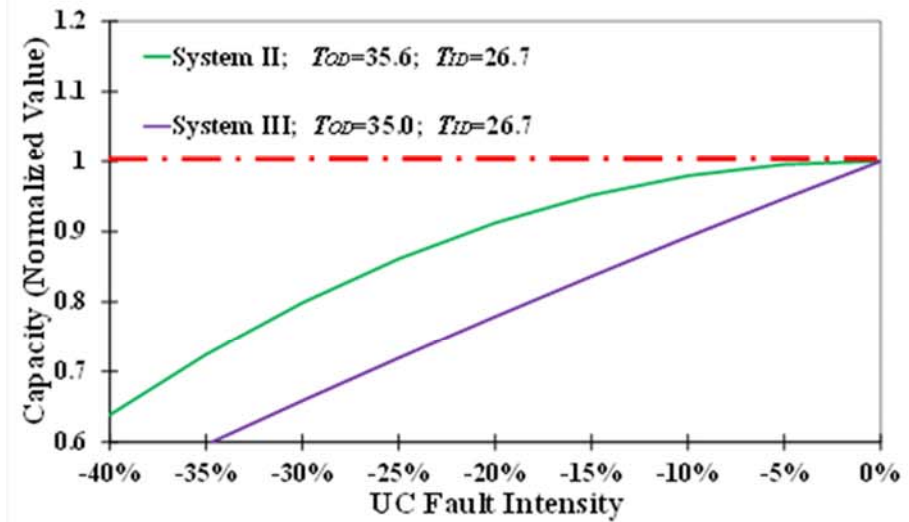


Figure 7

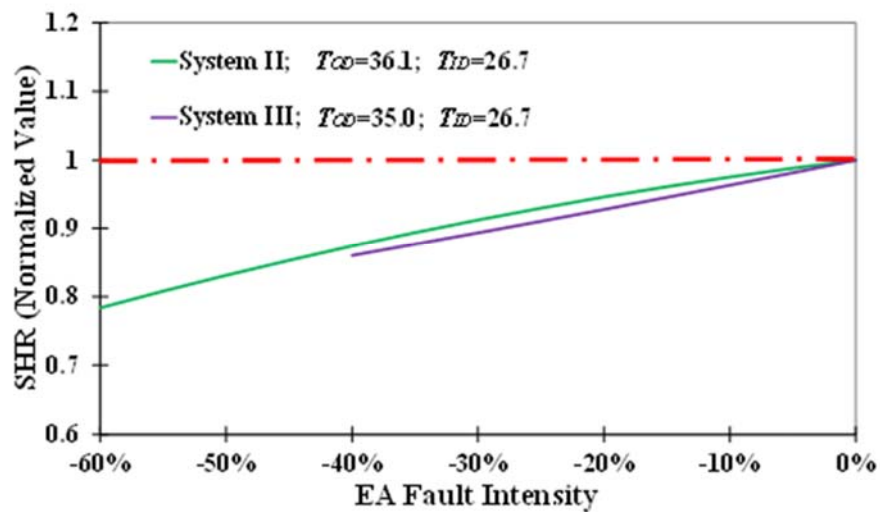
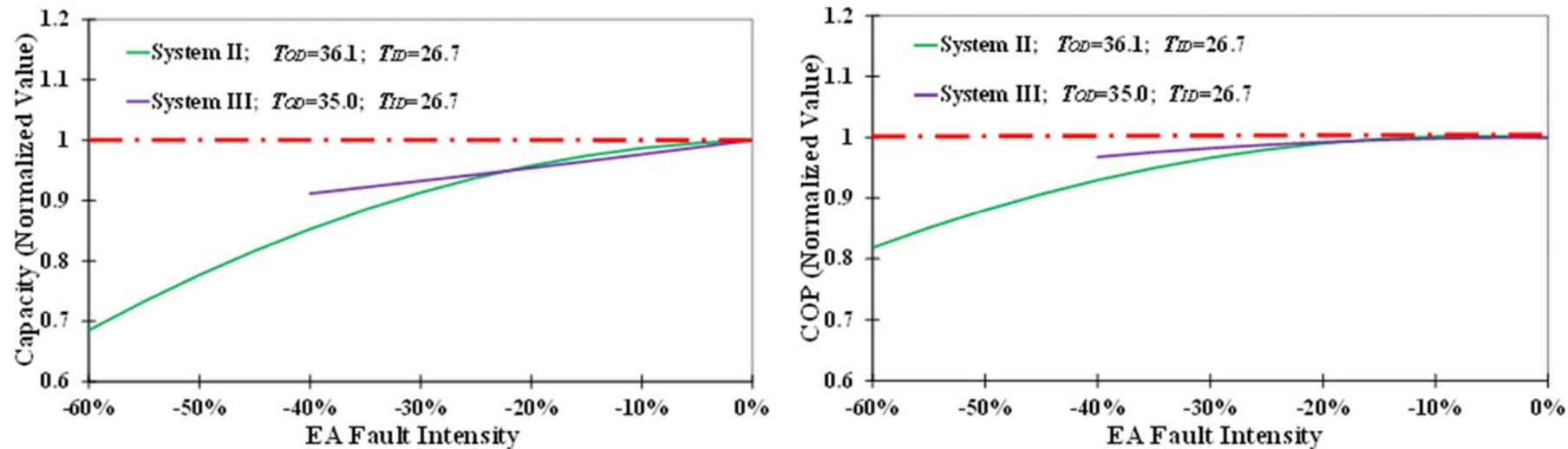


Figure 8

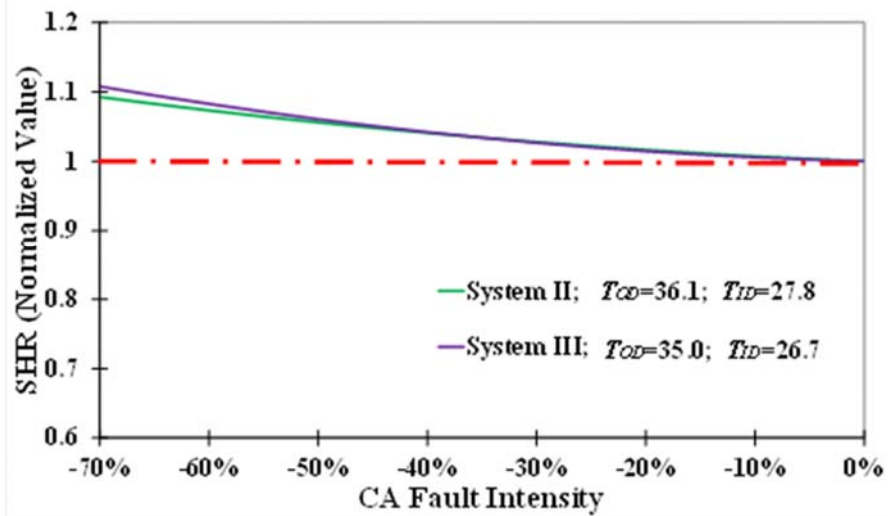
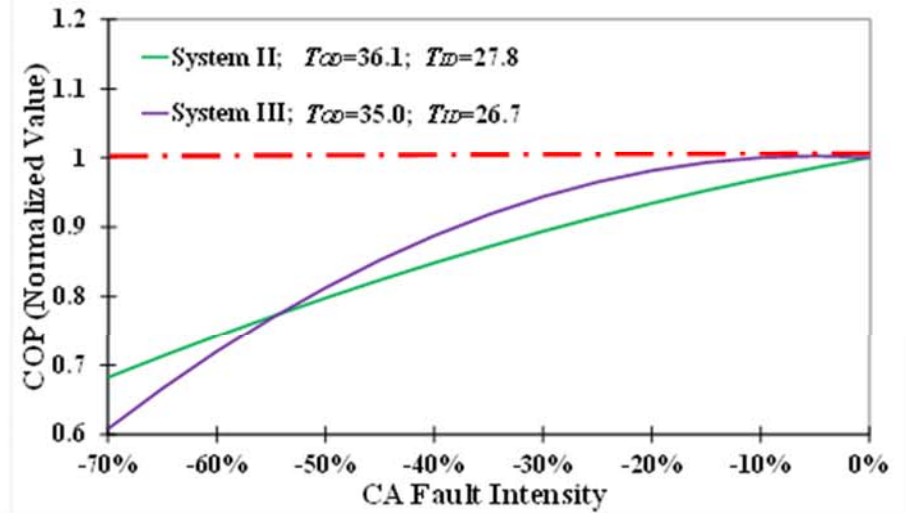
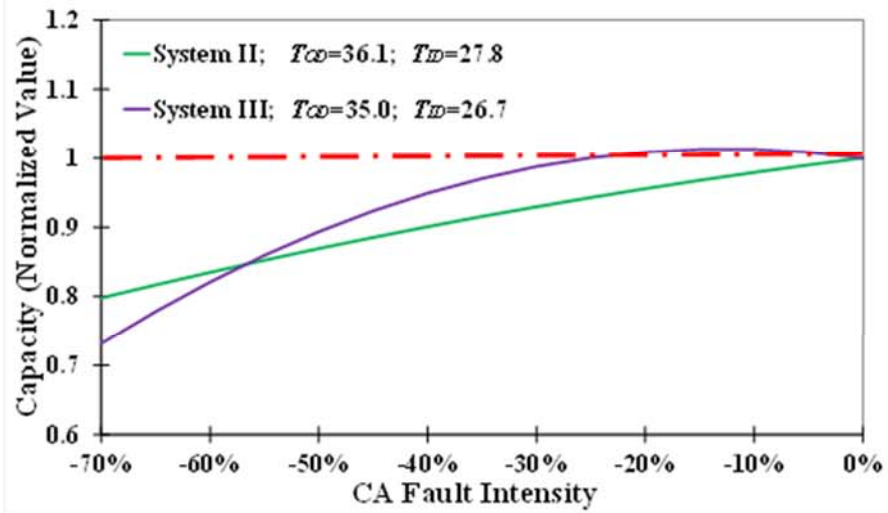


Figure 9

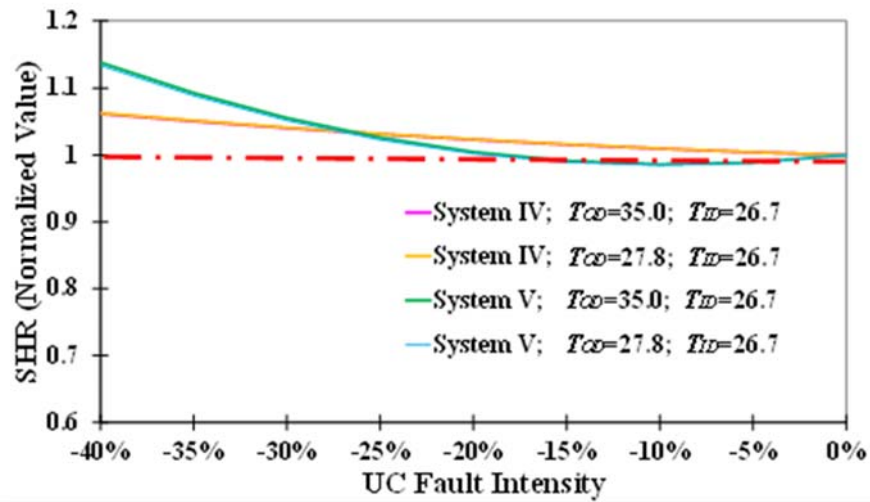
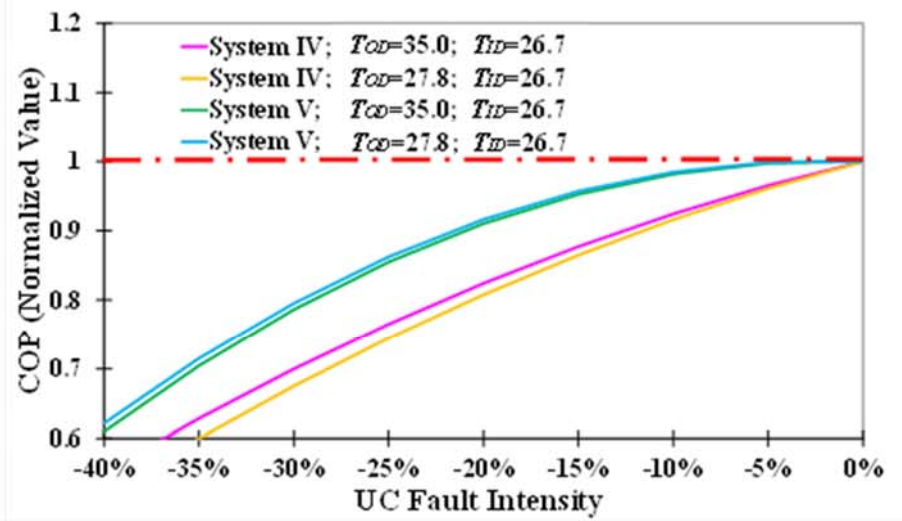
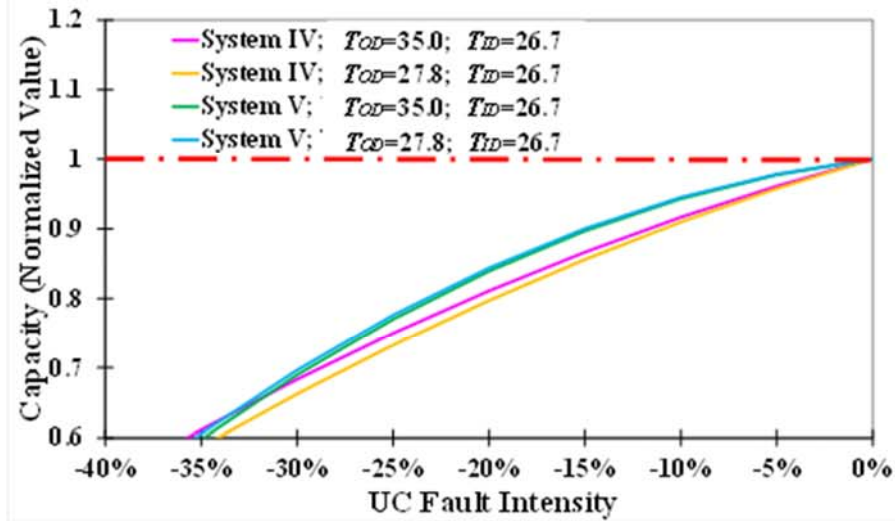


Figure 10

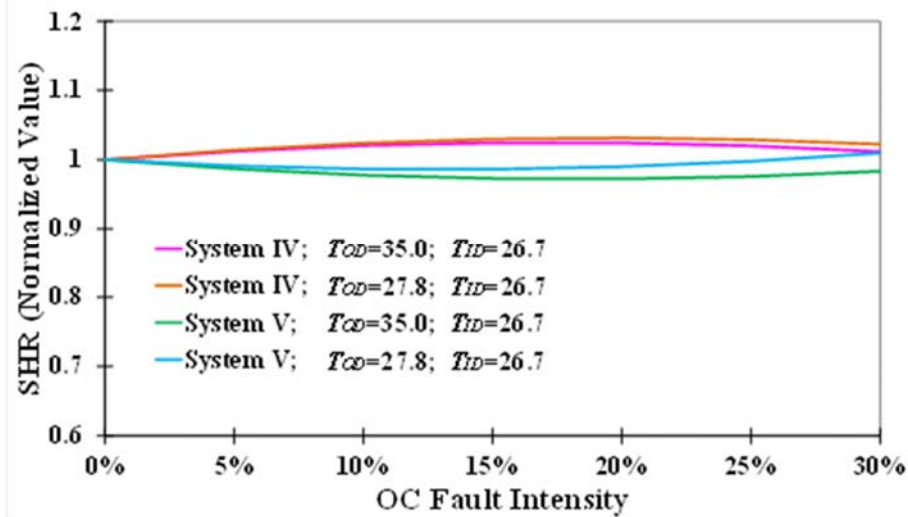
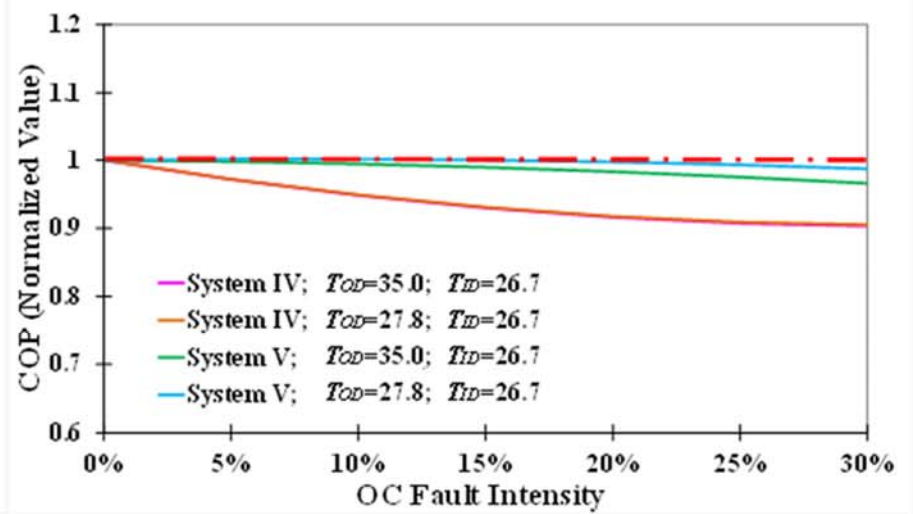
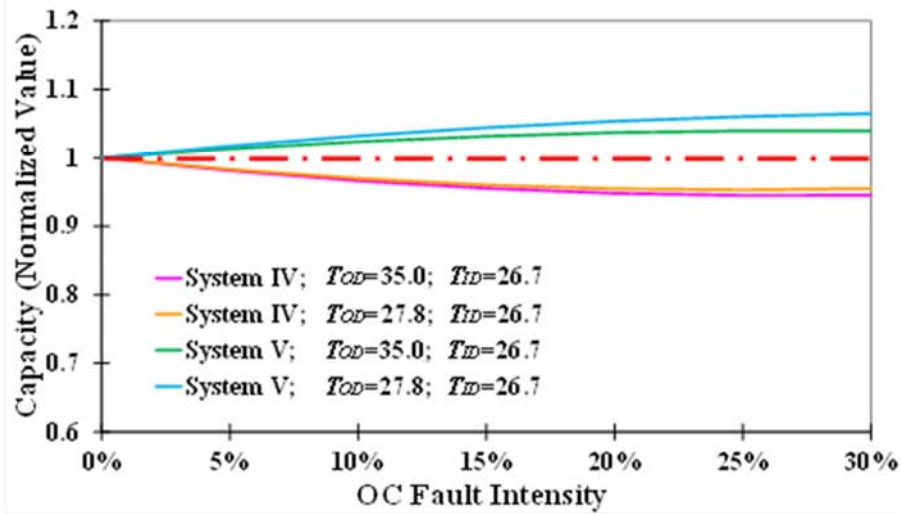


Figure 11

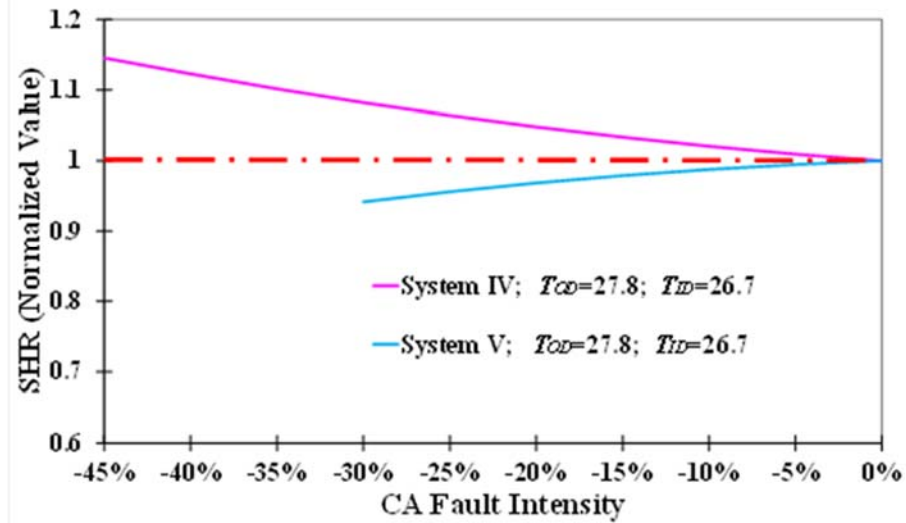
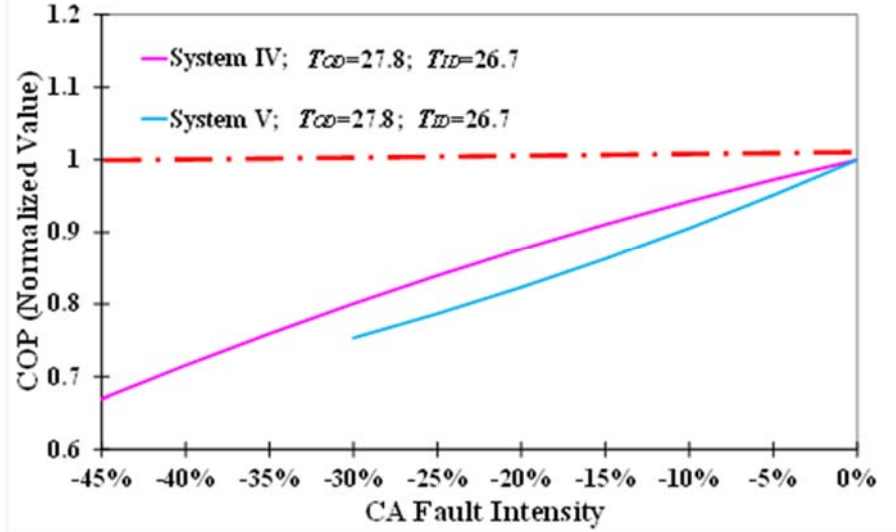
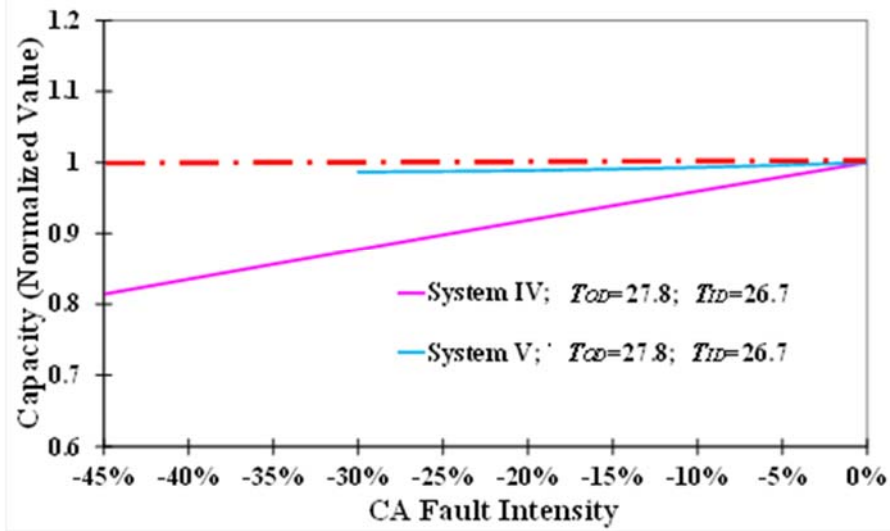


Figure 12